Mass Loss of Highly Irradiated Extra-Solar Giant Planets

by

Maki Funato Hattori

A Thesis Submitted to the Faculty of the

DEPARTMENT OF PLANETARY SCIENCES

In Partial Fulfillment of the Requirements
For the Degree of

MASTER OF SCIENCE

In the Graduate College

THE UNIVERSITY OF ARIZONA

2008

STATEMENT BY AUTHOR

This thesis has been submitted in partial fulfillment of requirements for an advanced degree at The University of Arizona and is deposited in the University Library to be made available to borrowers under rules of the Library.

Brief quotations from this thesis are allowable without special permission, provided that accurate acknowledgment of source is made. Requests for permission for extended quotation from or reproduction of this manuscript in whole or in part may be granted by the head of the major department or the Dean of the Graduate College when in his or her judgment the proposed use of the material is in the interests of scholarship. In all other instances, however, permission must be obtained from the author.

SIGNED: _____
Maki F. Hattori

APPROVAL BY THESIS DIRECTOR

This thesis has been approved on the date shown below:

_____ 7/25/08
Dr. William B. Hubbard, Professor of Planetary Sciences — Date

ACKNOWLEDGEMENTS

First and foremost I would like to thank my committee for their support. My advisor, William Hubbard for helping me work on the details of the project, Adam Showman for continuing to sit on my various committees after being the standing member, and Rory Barnes for being able to take the time from his busy baby-watching to give me revisions. I would like to thank the grad community at LPL for their support both academically and psychologically, especially my role-playing friends, Diana Smith, Dave Smith, Eric Palmer, Nicole Baugh, Kristin Block and Chris Schaller. I would also like to thank Serina Diniega, Abby Sheffer, Gwen Barnes, Eileen Chollet, Mandy Proctor, Stephanie Fussner, David Choi, Kelley Choi and Abraham Kuo for their help in working, not working and getting through graduate school.

I would also like to thank my family. My parents especially have always been a great inspiration to me as I was growing up and hope that I can someday repay them for all they have done for me. Last but definitely not least, most of all I would like to thank my fiancé, Brian Jackson, for his encouragement and his scientific opinions. I would not have been able to finish this thesis without him.

TABLE OF CONTENTS

LIST OF FIGURES

LIST OF TABLE

ABSTRACT

We present theoretical calculations for the evolution of highly-irradiated extrasolar giant planets. The value of the energy-limited escape rates are taken from Watson et al. (1981), Lammer et al. (2003) and Yelle (2004) which vary by two orders of magnitude. The lowest rate is from Watson et al., while the highest rate comes from Lammer et al., which predicts that all highly-irradiated planets are remnants of much larger planets. We find that for cases with lower mass loss rates, the tidal effects, such as the planet exceeding the Roche Lobe are more effective at removing mass than stellar radiation. We also compare our theories with observations to show observational evidence for mass loss.

CHAPTER 1: INTRODUCION

The discovery of the first extra solar giant planets (EGPs) were observed at distances very close to their parent star which came as a surprise to most scientists. As more data were gathered and more of these planets were discovered, their origin and development became a topic of great interest. In 2003, Vidal-Madjar and collegues found evidence for evaporation of HD 209458 b (Vidal-Madjar et al. 2003) when they observed an extended hydrogen atmosphere beyond the Roche lobe of the planet. Since stellar gravity and radiation would rapidly remove this mass, hydrodynamic escape must re-supply it. One theory of mass loss (Baraffe et al. 2004) predicts that HD 209458 b must be the remnant of a much larger planet because of this mass loss.

Studying EGPs will improve our understanding of the formation and evolution of planetary systems including the Solar System. One of the most striking difference between the Solar System and known planetary systems is the location of the planets. While in our own system large gaseous planets are located far from the star beyond 5AU, many of these other systems have large gaseous planets closer than Mercury is to our Sun. In addition the masses of EGPs, range up to 15 Jupiter mass (M_J) planets.

We can use the distribution of planetary masses to understand how planets form. This distribution is called the mass function and is described by the power law:

$$\frac{dN}{dM} \propto M^{-\alpha},$$

where M represents the mass of the planet, dN represents the number of planets in a mass bin of width dM, centered at M, and α is the index. Marcy et al. (2005) derived $\alpha = 1$ from the observations available at the time. If no effects have modified the masses of these observed planets then the current distribution would be the same as the distribution that the planets formed with. This special distribution is referred to as the initial mass function (IMF). In this thesis we discuss the effects of mass loss on planets and on the IMF.

In section 2 we discuss our methods and assumptions, in section 3 we show our results and finally in section 4 we discuss our conclusions and future work.

CHAPTER 2: METHODS & ASSUMPTIONS

In this thesis we consider different models for mass loss, also discussed in Hubbard et al. (2007a; 2007b). There are two common theories of mass loss: Jeans escape and hydrodynamic escape. If the distribution of the velocity of gas molecules in the atmosphere follows a Boltzmann distribution, with no bulk motion of the atmosphere, then a small fraction of the molecules, i.e. the ones with the highest velocities at the tail end of the Boltzmann distribution, have enough energy to escape the gravity of the planet, Jeans escape. Hydrodynamic escape results from the bulk motion of the atmosphere radially outwards. For the planets that we are considering, hydrodynamic escape is the dominant form of mass loss and thus we do not specifically consider Jeans escape. Mass loss is energy-limited, i.e. a significant fraction of the available energy goes towards the molecules escaping from the planet. For energy-limited escape, the escape rate Φ (molecules cm^{-2} s^{-1}) is proportional to the volumetric heating rate of the atmosphere from stellar extreme-ultra-violet (XUV) radiation, Q_0 (erg cm^{-3} s^{-1}).

The proportionality constant between the two factors includes a great deal of complexity including chemistry, absorption rate and cooling rate which we parameterize as ε, the efficiency factor. ε is given by the following expression:

$$\varepsilon = \frac{\Phi E_B}{S_*},$$

where E_B be the binding energy of a molecule at 1 bar such that $E_B = mV_0$, where V_0 is the gravitational potential, m is the molecular mass and S_* the stellar flux at semi-major axis, a. If mass loss were perfectly efficient, then all of the incoming XUV radiation would be converted to kinetic energy of the molecules. This situation would correspond to ε=1. In reality for energy-limited escape some fraction of the XUV photons impart kinetic energy greater than the binding energy to the molecules, corresponding to ε <1.

Φ also depends on the mass of the planet, the radius of the planet, the mass of the star, the semi-major axis, the current time, the elemental composition etc., i.e. $\Phi = \Phi(M_p, R_p, M_*, a, t, Z, \varepsilon, \ldots)$. In our model we consider how a planet's properties evolve with time due to the effects of the gravity of the star (section 2.1), the change in XUV flux from the (section 2.2), the evolution of the planet (section 2.3), and the efficiency, ε, (section 2.4). Given a planet's initial conditions (section 2.5) we are able to calculate parameters, including the mass, over time incorporating these effects.

Our approach is not to generate independent mass loss efficiencies, but rather to parameterize mass loss models in terms of ε. By employing this simple parameterization we can compare the results of different ε values and their observational consequences. We do not consider the possibility of changing ε over time because we find that most mass loss occurs over a short time span.

2.1 Tidal effects on atmospheric binding

For planets far from the host star the kinetic energy required for a molecule to escape can be approximated as $E_B = mV_0$. However, when the planet is close to the star, the star's gravity reduces the amount of kinetic energy required to escape from the planet. Unlike in an isolated case where a molecule would have to escape to infinity to become unbound, we consider a molecule unbound once it is beyond the Hill radius of a planet (i.e. when it exits the gravitational influence of the planet). Thus we assume the binding energy is zero at the star's L1 Lagrange point. So we define a modified binding energy:

$$E_{B,\,mod} = mV_{mod}(r) - mV_{mod}(r=L1) = m\Delta V_{mod},$$

where V_{mod} is the modified gravitational potential in the planet's frame of reference as a function of distance from the planet's center, r. When the radius of the planet, r, exceeds the L1 distance then we consider the planet to be completely evaporated. We choose a solar type star of 1 Solar Mass (the Sun) for our model. In general, for the same size planet a larger star would decrease the binding energy while a smaller star would increase the binding energy.

2.2 Time evolution of stellar illumination

Observations have shown that young stars are very magnetically active (Ribas et al. 2005). As they age, their rotation rates slow and consequently the magnetic dynamo activity drops off, reducing the XUV emission. In order to approximate the time evolution of the stellar XUV flux, $S_*(t)$, we use the observed power law:

$$\frac{S_*(t)}{S_*(4.5Gyr)} = \left(\frac{4.5Gyr}{t}\right)^{1.23}.$$

This equation reproduces the strong XUV flux of stars at early ages and the declining flux at later times.

We start our mass loss calculations when the star is 10^6 years old, presumably migration (Lin et al. 1996) and the nebula is dissipated (Bell et al. 1997). In our scenario planets are formed far from the parent stars and migrate inwards due to interactions with the nebula (Lin et al. 1996; Trilling et al. 1998; Ida et al. 2004). Before the nebula dissipates at 10^6 years, the proto-planet is shielded from the stellar flux (Bell et al. 1997), giving an effective efficiency, $\varepsilon = 0$. We assume that the irradiated giant planets are deposited at their currently observed semi-major axis by gas disc migration and do not experience any further movement. There is some variation in the dissipation time scale of the nebula but we have selected an average value. As the equation clearly indicates starting the model at an earlier time increases the total amount of mass lost because the XUV flux is so much higher at earlier times.

Recently there has been some evidence that migration post dissipation of the proto-planetary nebula might be significant (Jackson et al. 2008a). If true, then the effects of mass loss would potentially be different from what we discuss here (see section 4).

2.3 Interior Evolution

Another important aspect of our model is the interior evolution of the planet. As the planet ages, it cools to space, reducing the internal entropy, and the planet's radius contracts (Hubbard 1984). To model the evolution, we integrate the equations of structure. First we create a grid of evenly spaced mass shells $M(r)$ and create a arbitrary mass density for each of these mass shells, $\rho = \rho(M)$. We can now solve for the radius r of each mass shell by integrating:

$$\frac{4\pi}{3} r^3 = \int_0^{M(r)} \frac{dM'}{\rho}.$$

Now we solve for the pressure, $P(r)$, in each shell by solving:

$$P(r) = P_{central} - \int_0^{M(r)} \frac{GM'\,dM'}{4\pi r^4}.$$

We now refer to our chosen equation of state, in this case the Saumon equation of state (Saumon et al. 1995) for planets of solar composition, to solve for $\rho(P)$ for each mass

shell. We now go back to calculating the radius *r* of each mass shell and repeat the following steps until the solution converges.

After we have found the radius, we can calculate the surface gravity of the planet. Using the surface gravity and the current interior entropy we can determine the effective temperature, T_{eff}, of the planet by using a surface condition grid (Burrows et al. 2004). Since our model steps in entropy steps, T_{eff} allows us to calculate the time step, dt, corresponding to the entropy step, dS, by using:

$$dt = \frac{T_{average} M}{4\pi r^2 \sigma T_{eff}^4} dS,$$

where σ is the Stephan-Boltzmann constant, M is the planetary mass, $T_{average}$ is the average temperature of the planet, and r is the radius of the planet. In Figure 1 we show the evolution of a planets entropy, *S/Nk*, surface gravity, *g*, and T_{eff},. As discussed previously, the internal entropy of the planet drops over time, the planet cools (i.e. T_{eff} decreases) and the planets radius shrinks (i.e. *g* increases). While the internal evolution of planets with different initial conditions differs quantitatively from this figure the qualitative behavior of all of the planets modeled here are represented by this figure.

Figure 1: Evolution of a 1 M_J planet along a surface grid for a = 0.046 and $\varepsilon = 10^{-6}$

The red line represents the evolution of the planet over time along the surface grid. This surface grid is specifically for a = 0.046 AU and illustrates the relationship between the planet's specific entropy, S/Nk, the log of the planet's surface gravity, g and effective temperature, T_{eff}. S/Nk is unitless (S represents the total entropy of the planet, k represents Boltzmann's constant and N represents the total number of particles in the planet), g is in cm^2/s and T_{eff} in Kelvin.

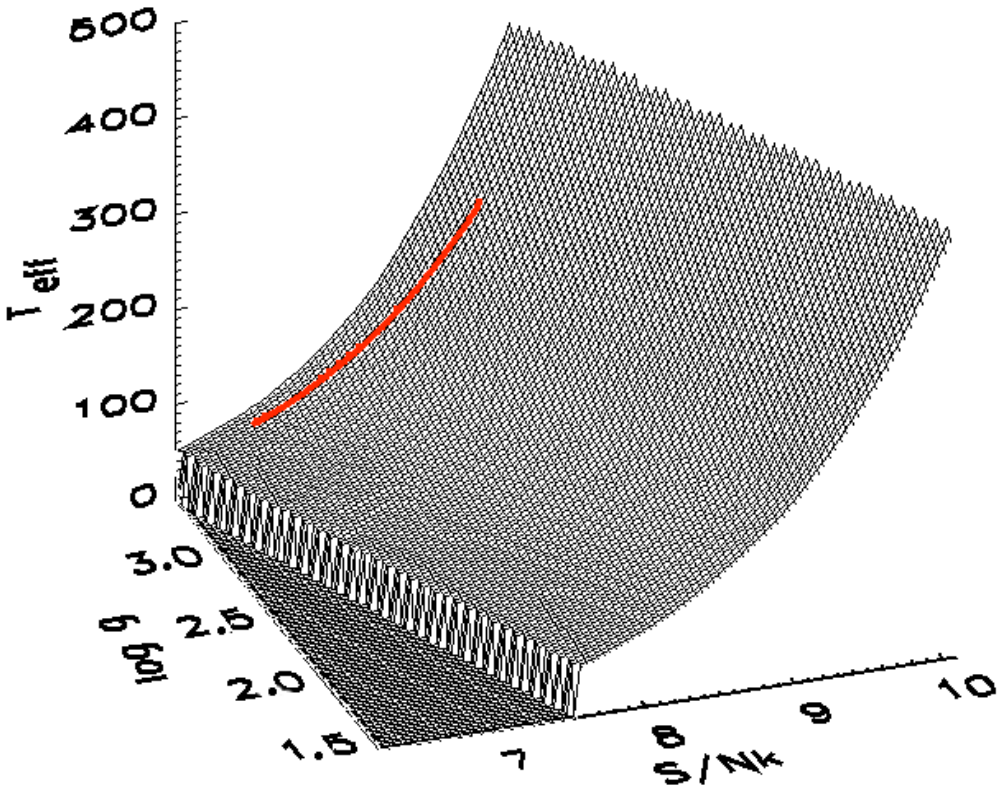

2.4 Efficiency Values

In order to choose values of the efficiency parameter, ε, we use three different mass loss models (Watson et al. 1981; Lammer et al. 2003; Yelle 2004). These models correspond to ε values that span two orders of magnitude ranging from $10^{-6} \leqq \varepsilon \leqq 10^{-4}$.

The least efficient model was originally developed by Watson et al. (1981) as an analytic hydrodynamic escape model for the Earth, a terrestrial planet with a hydrogen exosphere at 1 AU from a solar type star. In this model, all of the XUV is absorbed at a specific altitude, and the energy is transferred by conduction to other parts of the exosphere. The efficiency, $\varepsilon = 10^{-6}$, results from their assumption that 1 erg cm^{-2} sec^{-1} of the Solar constant ($1.4 * 10^{6}$ erg cm^{-2} sec^{-1}) is converted to molecular kinetic energy.

The most efficient model (Lammer et al. 2003; Baraffe et al. 2004), $\varepsilon = 10^{-4}$, is based on an analytic approach similar to Watson's work. However, this model contains no chemical effects as the authors suggest that there in not enough production of H_3^+ ions for the radiative cooling to be a significant effect on the total heating rate. The authors have since decided that this efficiency is erroneous but we continue to use the value to illustrate what features an efficient case of mass loss would demonstrate.

Yelle's numerical model was developed to study mass loss from close-in giant planets (Yelle 2004, 2006). It is unique from the other models because it explicitly includes chemical effects in the upper atmosphere. Some of the XUV flux is lost to the formation of H^+ and the radiative cooling from the H_3^+. Yelle's model incorporates an atmospheric heating profile for which the volumetric heating rate varies with altitude, however, it does not incorporate any possible tidal enhancement effects nor does it consider the time evolution of the stellar flux or the planet. From Figure 7 of Yelle 2004, we estimate $\varepsilon=5*10^{-6}$.

2.5 Monte Carlo Initial Conditions

In order to determine if the close-in planets have a different mass function than the planets further out, we performed a Monte Carlo integration of the mass loss model. First, to develop an empirical initial mass function (IMF), we divide the observed EGPs into two groups: "irradiated planets"(close enough to experience mass loss: within 0.07AU of their star) and "field planets" (beyond 0.07 AU). Hubbard et al. (2007a) show that field planets experience negligible mass loss and the distribution of their masses would be unchanged since their formation, thus equivalent to the IMF. Using the same bin size as Marcy et al. (2005) our independent fit to the "field" planet mass function gives us α = 1.19, this value was derived from the reported EGPs listed on the Extrasolar Planets Encyclopedia located at http://exoplanet.eu. Thus we select the initial mass randomly

from the derived IMF distribution, evolve the planet, and can construct an “irradiated” MF to compare to the IMF as seen in section 3.4.

We create an “irradiated” MF for four semi-major axes. We chose the distances 0.023 AU and 0.046 AU because they are the semi-major axis of OGLE-TR-56 b and HD 209458 b, respectively. 0.034 AU was chosen to be between 0.023 and 0.046 AU and we chose 0.057 to be 0.011 AU further than 0.046AU, the same separation as the other distances. These four distances each have a different evolutionary grid (section 2.3) associated with them and show distinctive differences in evolution between them.

CHAPTER 3: RESULTS & DISCUSSION

3.1 5 Jupiter Mass (M_J) planets

Below we present the mass, radius and loss rate calculated for a planet with a starting mass of 5 Jupiter Masses at the four orbital distances for different efficiencies. These models are not intended to be for any particular planet but to show the general tendencies and differences between the models.

Figure 2: Mass vs. Time for three efficiencies for planets starting at 5 M_J

Mass vs. time for three different efficiencies, ε. The solid lines are for a planet at an orbital distance of 0.023 AU, the dotted lines are for 0.034 AU, the dashed lines are 0.046 AU and the dash-dotted lines are 0.057 AU.

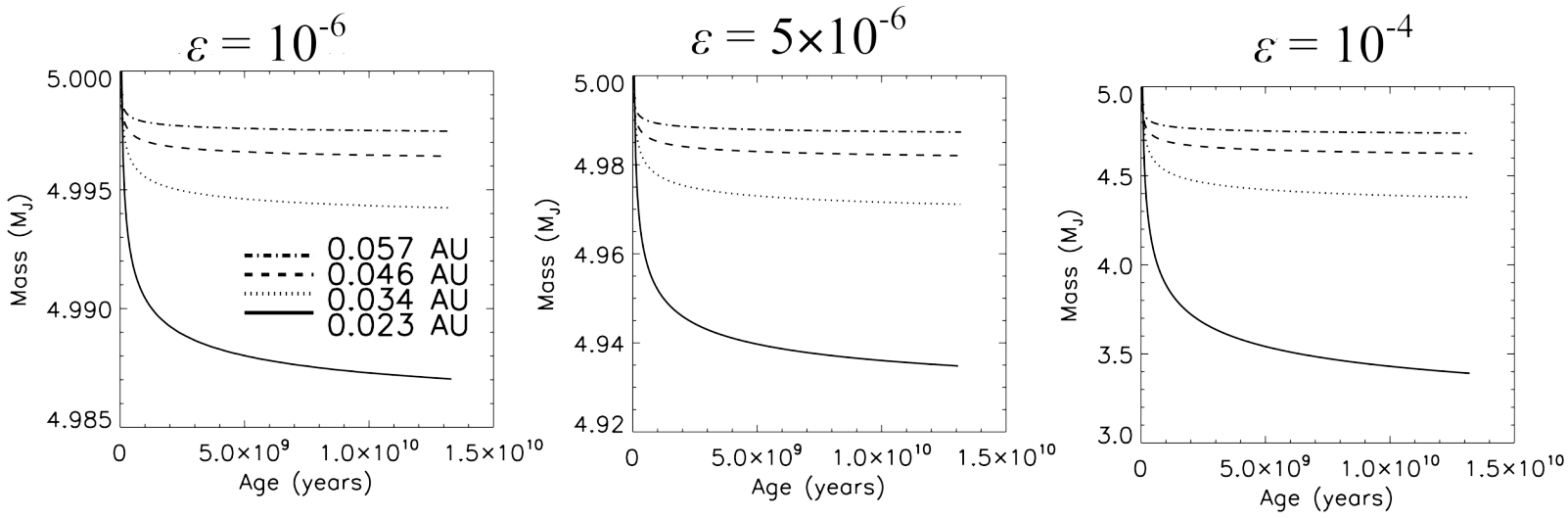

Figure 3: Radius vs. Time for three efficiencies for planets starting at 5 MJ

Radius vs. time for three different efficiencies, ε. The solid lines are for a planet at an orbital distance of 0.023 AU, the dotted lines are for 0.034 AU, the dashed lines are 0.046 AU and the dash-dotted lines are 0.057 AU.

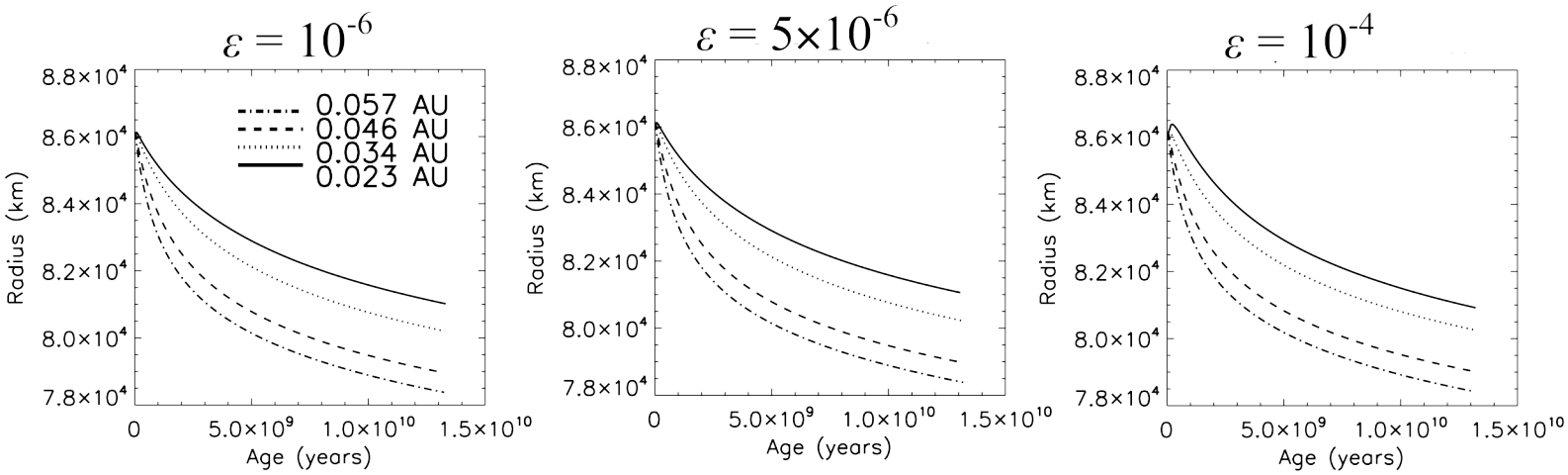

Figure 4: Mass Loss vs. Time for three efficiencies for planets starting at 5 M_J

Mass Loss vs. time for three different efficiencies, ε. The solid lines are for a planet at an orbital distance of 0.023 AU, the dotted lines are for 0.034 AU, the dashed lines are 0.046 AU and the dash-dotted lines are 0.057 AU.

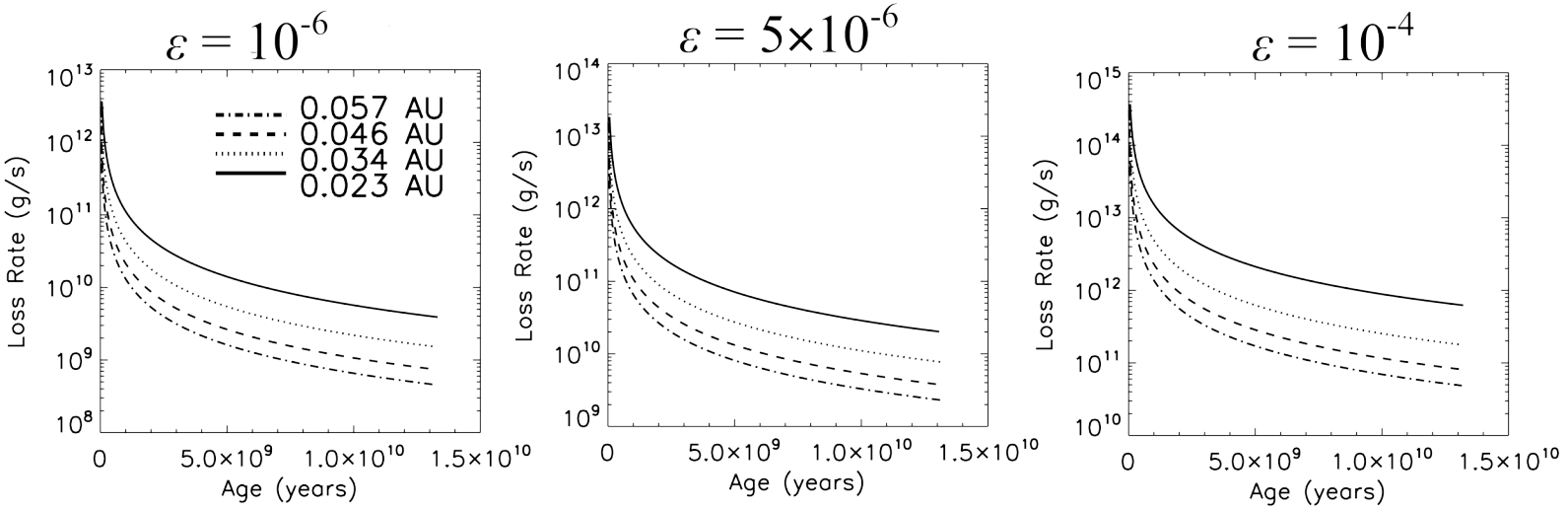

From the graphs we can see that all the models show the same basic shape, for mass, radius and mass loss. Figure 2 shows mass as a function of time for three different efficiencies, ε. In general the mass decreases with time and with increasing distance. As expected, most of the mass loss occurs at early times and the higher efficiencies exhibit larger mass loss. In the two lower efficiency models, the final mass after 13 Gyrs is still approximately 5 M_J with less than 1% loss on all but one simulation, while in the high efficiency model, the closest planet loses 30 % of its initial mass. For example, the planet CoRoT-Exo-2, with a mass of 3.3 M_J located at 0.028 AU (Alonso et al. 2008), would have had to start as a $5M_J$ planet if $\varepsilon = 10^{-4}$, but such an increase is not necessary for lower efficiencies.

We can see from Figure 3 that the radius of the planet is not significantly affected by the different mass loss efficiencies, which is not surprising since the radii of hydrogen rich planets in the Jupiter mass range are insensitive to the mass (Hubbard 1984). However, the radius is affected by irradiation from the star, and hence closer-in planets maintain a larger radii (Burrows et al. 2004).

The mass loss rates in Figure 4 show similar trends with mass loss rates falling by orders of magnitude over time, but are quantitatively different, as we would expect. Mass loss rate decreases due to the decrease of the stellar XUV flux and the increase of the binding energy as the planet contracts.

3.2 1 Jupiter Mass models

Below we present the mass, radius and loss rate for a planet with a starting mass of 1 Jupiter Mass for the models. All of the highest efficiency models, $\varepsilon = 10^{-4}$, are omitted on the graphs because the planets do not survive the early, high irradiation from the star and evaporate away in the first few ten million years. The $a = 0.023$AU, $\varepsilon = 5*10^{-6}$ model is omitted from the collective plot and discussed later.

Figure 5: Mass vs. Time for two efficiencies for planets starting at 1 M_J

As in Figure 2, mass vs. time for different efficiencies, ε. The solid lines are for a planet at an orbital distance of 0.023 AU, the dotted lines are for 0.034 AU, the dashed lines are 0.046 AU and the dash-dotted lines are 0.057 AU.

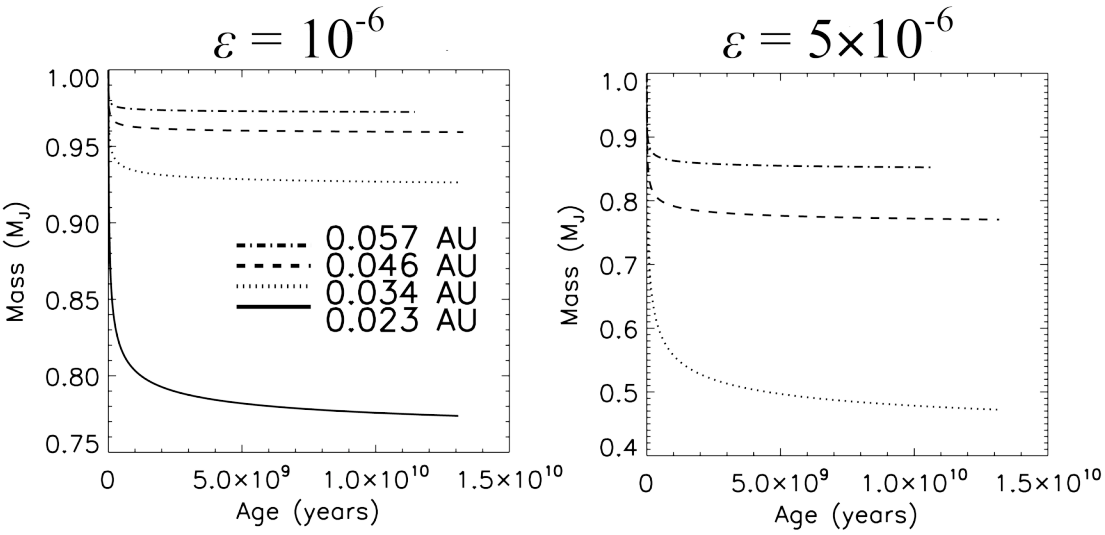

Figure 6: Radius vs. Time for two efficiencies for planets starting at 1 MJ

As in Figure 3, radius vs. time for different efficiencies, ε. The solid lines are for a planet at an orbital distance of 0.023 AU, the dotted lines are for 0.034 AU, the dashed lines are 0.046 AU and the dash-dotted lines are 0.057 AU.

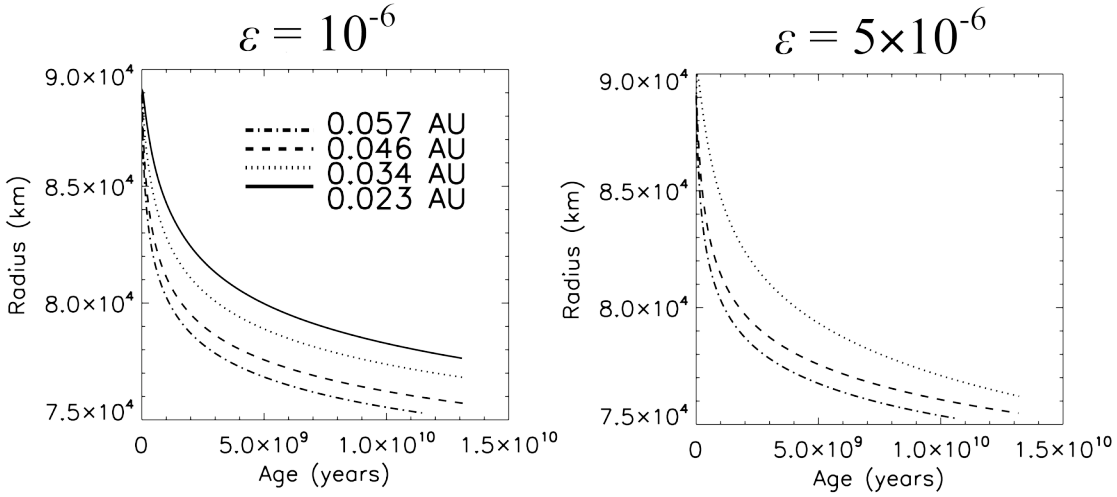

Figure 7: Mass Loss vs. Time for two efficiencies for planets starting at 1 MJ

As in Figure 4, mass loss vs. time for different efficiencies, *ε*. The solid lines are for a planet at an orbital distance of 0.023 AU, the dotted lines are for 0.034 AU, the dashed lines are 0.046 AU and the dash-dotted lines are 0.057 AU.

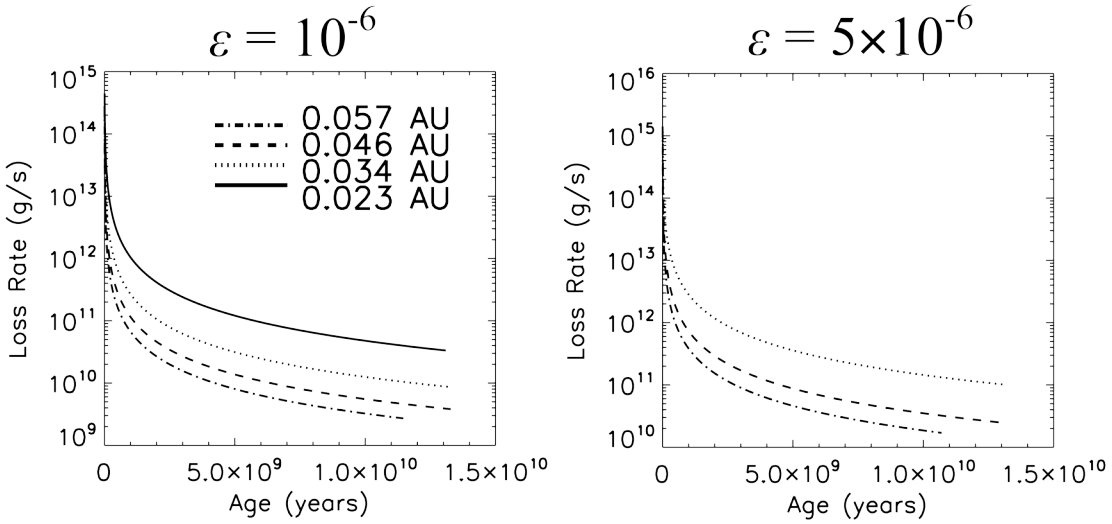

We can see that the trends in Figure 5 are similar to those in Figure 2. Most of the mass loss occurs at the early times, with the a = 0.023 AU, $\varepsilon = 10^{-6}$ simulation losing over 20% of the initial mass and the a = 0.034 AU, $\varepsilon = 5*10^{-6}$ simulation losing over 50% during the 13 Gyrs. Figure 6 and Figure 7 continue to illustrate the importance of the semi-major axes and the efficiency parameters as Figure 3 and Figure 4 do.

Comparing these results to the results from the 5 M_J model, we see that smaller masses tend to lose more mass than larger planets. The exospheres of these smaller planets are not as tightly bound as their larger mass counterparts and loose more mass.

For a = 0.023 AU, $\varepsilon = 5*10^{-6}$, the simulation exits during the fifth time step because the planetary mass has dropped below zero. Planets with these parameters do not survive much longer than the gas disk. This total evaporation is also true of the 1 M_J, $\varepsilon = 10^{-4}$ cases. We neglect the effects of a core but, it is possible that an icy-rock remnant core of several earth masses might remain (Raymond et al. 2008).

3.3 Initial masses with 50% retention at 5 Gyrs

Table 1 shows the initial mass of a planet for which 50% of the mass is lost after 5 Gyrs of evolution. For example for a = 0.023 AU, $\varepsilon = 10^{-6}$, a planet that starts with 0.82 M_J

would be 0.41 M_J after 5 Gyrs. In section 3.3, we showed that smaller mass planets lose a higher percentage of their initial mass. So given an initial semi-major axis, planets with masses less than the value in the table would lose more than 50% of their initial mass. For example for $\varepsilon = 10^{-6}$, a 1 M_J planet at a = 0.023AU would lose less than 50% of its initial mass.

Table 1: Initial mass of a planet which experiences 50% loss after 5 Gyrs

Semi-major axis	$\varepsilon = 10^{-6}$	$\varepsilon = 5*10^{-6}$	$\varepsilon = 10^{-4}$
.023 AU	.82 M_J	1.5 M_J	4.6 M_J
.034 AU	.56 M_J	.92 M_J	3.2 M_J
.046 AU	.44 M_J	.79 M_J	2.7 M_J
.057 AU	.37 M_J	.72 M_J	2.3 M_J

If $\varepsilon = 10^{-4}$, then all of the smaller mass planets are remnants of giant planets for high efficiency, $\varepsilon = 10^{-4}$, only the smallest planets are remnants for the lower efficiencies. Given the observational data, the high efficiency model implies that planet formation is quite common and there used to be significantly more planets than we can currently observe.

3.4 IMF versus models and observations

To look for evidence of mass loss amongst the "irradiated" planets, we compare them relative to the IMF derived from the "field" planets. Such a comparison depends sensitively on the bin size. Many of the planets that lose significant mass are less than 1 M_J, so, if we continue to use $dM = 1\ M_J$, then we would combine planets that lose significant amounts of mass with those that do not. Thus we chose $dM = 0.3\ M_J$ in order to have a finer bin size to observe these details and yet retain a statistically significant number of planets in each bin. Using the revised binning gives us an IMF with $\alpha = .60 \pm .04$, shown as the solid line in Figure 8 along with the observed "field" mass distribution. To this newly revised IMF, we will compare the "irradiated" planets and the theoretical distributions for different efficiencies and distances.

Figure 8: IMF binned in 0.3 M_J bins

Revised fit to the observed "field" planets when the "field" planets are divided into bins of dM = 0.3 M_J.

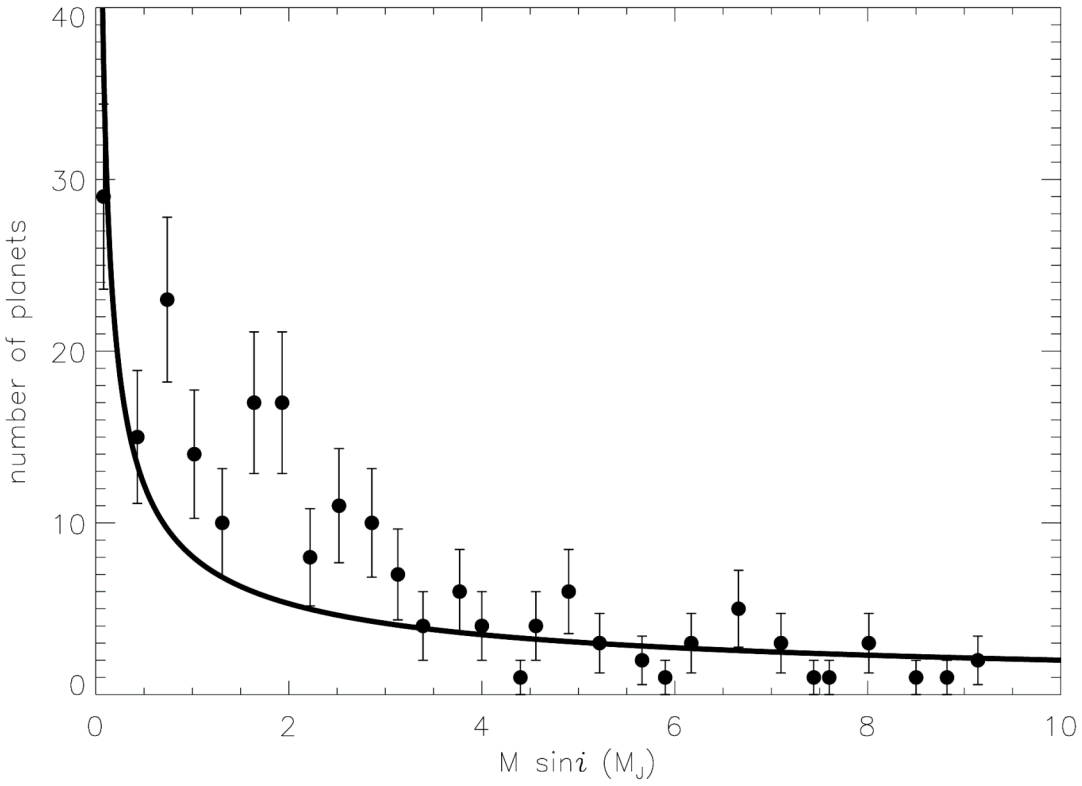

Figure 9: Mass distributions of models relative to the IMF

The thick black line labeled IMF represents the revised IMF for the field planets discussed previously (α = 0.6). Predicted mass functions for EGPs over 5 Gyrs for the three different efficiencies are color-coded: $\varepsilon = 10^{-6}$ is shown in black, $\varepsilon = 5*10^{-6}$ is in red, and $\varepsilon = 10^{-4}$ is in green. The different line styles indicate orbital distances as in the previous figures. The dots are the currently observed distribution of highly-irradiated giant planets out to 0.07 AU. All of the distributions here are normalized to 1 planet at 1 M_J.

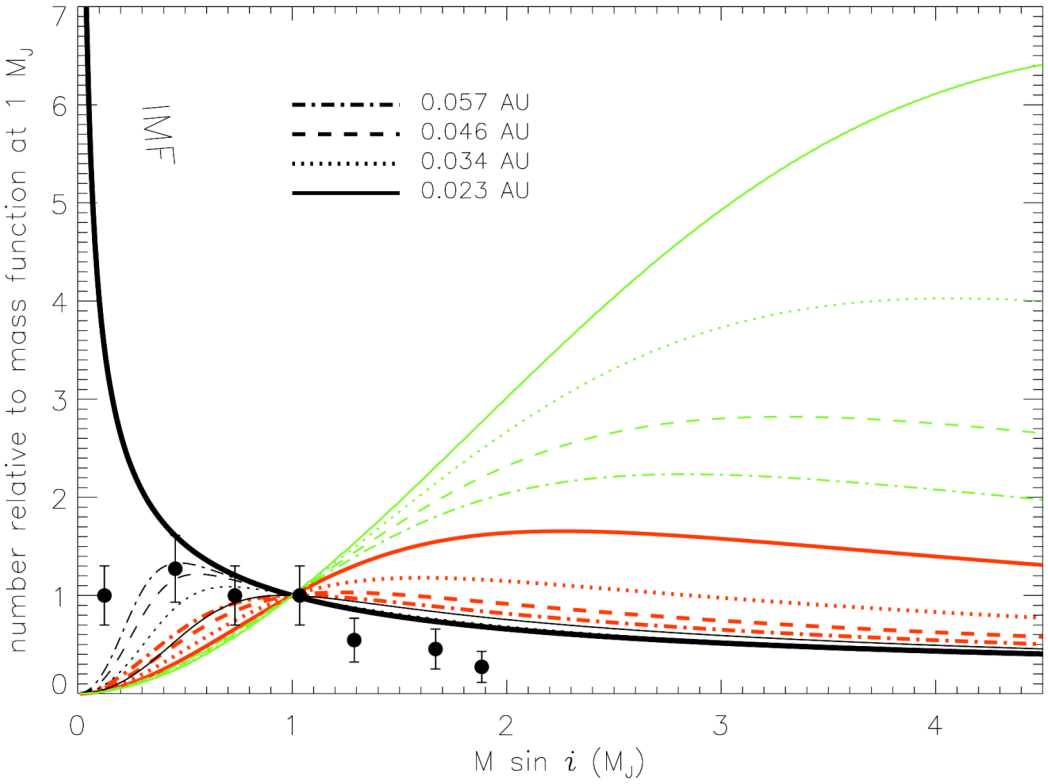

In Figure 9, the IMF is the best fit initial mass function for the "field" planets binned in 0.3 M_J bins. It represents a power law with exponent $\alpha = .60$. The other lines are the smoothed analytical fits to the results of evolving the IMF with different efficiencies and distances. The green lines represent $\varepsilon = 10^{-4}$, red lines represent $\varepsilon = 5*10^{-6}$, and black represent $\varepsilon = 10^{-6}$. The lines are normalized such that all of the models have the same value at 1 M_J. If there were no mass loss, the analytical fit would coincide exactly with the IMF.

The dots represent the observed mass distribution of planets closer than 0.07 AU, derived from data given in Appendix A. The observed distribution is normalized in the same way as the analytic distributions. The bin width is 0.3M_J.

In the figure we see that the dot representing the lowest mass bin shows disagreement from the IMF, indicating that there is a deficiency in the abundance of lowest mass planets. The disagreement is at the 1.56σ level which suggests that the disagreement is statistically significant but not necessarily conclusive. This disagreement is likely the result of mass loss of the lowest mass planets, and the agreement between the observed mass distribution and the prediction of the $\varepsilon = 10^{-6}$ model corroborates this hypothesis.

The fit to the $\varepsilon = 10^{-4}$ model predicts less small mass planets than are actually observed. Unless the initial mass function of "irradiated" planets is inherently different than that of

"field" planets, then this efficiency is inconsistent with observations. Thus we conclude that the mass loss efficiency is probably of order 10^{-6}.

Figure 10: Mass distributions of models relative to the IMF

The thick black line labeled IMF represents the revised IMF for the field planets discussed previously (α = 0.6). Predicted mass functions for EGPs over 5 Gyrs for the three different efficiencies are color-coded. $\varepsilon = 10^{-6}$ is shown in black, $\varepsilon = 5*10^{-6}$ is in red, and $\varepsilon = 10^{-4}$ is in green. The different line styles indicate orbital distances as in the previous figures. The dots are the currently observed distribution of highly-irradiated giant planets out to 0.15 AU. All of the distributions here are normalized to 1 planet at 1 M_J.

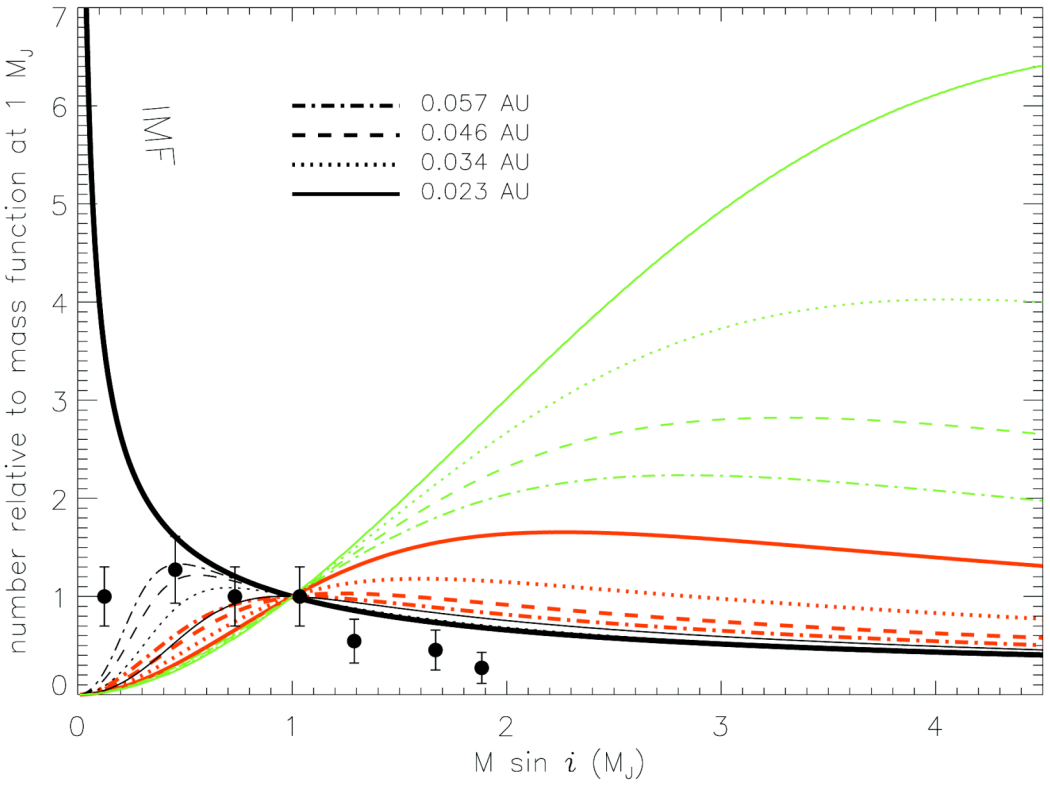

Figure 10 is the same as Figure 9 but with the cut-off semi-major axis of the observed planets set at 0.15 AU rather than 0.07 AU. We see that the deficiency in the smallest mass bin is still present.

It is important to remember that we are plotting Msin*i* of the planet and not the actual masses since for most planets they are unknown. Assuming the inclinations are randomly oriented, the sin*i* degeneracy should not significantly affect our close-in distributions (Hubbard et al. 2007a). Smaller mass planets are more difficult to find using radial velocity surveys so we believe there may be inherent observational biases in the data (Wittenmyer et al. 2006). However, we believe that this observational bias does not affect our primary result. Since it is more difficult to observe a planet that is further away, we would be more likely to be missing small "field" planets rather than "irradiated" planets. Consequently the deviation from the IMF would become even more prominent as radial velocity surveys become more complete.

CHAPTER 4: CONCLUSIONS & FUTURE WORK

In this thesis we have shown that mass loss can be a significant effect for some planets close-in to their parent stars, especially those in the lower mass ranges. We compare the "field" planets to the "irradiated" planets and verified that there is some observational indications of mass loss. Our Monte Carlo simulations verified that an efficiency of $\varepsilon \sim 10^{-6}$ can explain the observed masses of close-in planets, assuming they began with the same IMF as the field planets.

If the IMF of close-in EGPs were enhanced in planets between 2 M_J and 5 M_J relative to "field" planets then an efficiency of 10^{-4} might be consistent with the current mass function of "irradiated" planets. If there was a mass range that preferentially underwent orbital migration, then the initial mass functions of the "field" and "irradiated" planets would be different. However, there has not been any consensus yet about whether there is a mass dependence (Ida et al. 2004; Del Popolo et al. 2005).

Future work should incorporate other important effects into the mass loss model. For example, if planets experience significant tidal migration due to star-planet interactions (Jackson et al. 2008a) after the initial orbital migration from gas-planet interactions, mass loss rates over time might be significantly different from our results here. For example, a $5M_J$ planet that tidally migrates from 0.046 AU to 0.023AU would lose less mass than a $5M_J$ planet that has been at 0.023AU for the same period. The tidal migration effect is

only important within ~0.2 AU, so it would not affect the field planets. However, for a given eccentricity, higher mass planets would undergo faster tidal migration, so the tidal effects on mass loss rates might be more pronounced for planets with higher masses.

The tidal heating of the planet would inflate the radius of a planet (Jackson et al. 2008b; Liu et al. 2008) making the upper atmosphere less tightly bound. To first order, for any initial mass and efficiency, we would expect more mass to be lost from all models after these effects of tidal heating are incorporated.

We have assumed that all of these planets are made of a solar composition of hydrogen and helium. If a planet had a significantly different composition, it would be governed by a different equation of state than the one we have used. And consequently it would undergo a different evolution. We might expect that a planet composed of heavier elements would undergo less mass loss than a planet of the same mass made of our assumed composition. Modeling the effects of different composition on mass loss rate should also be the subject of future work. As more planets are discovered, our analysis can be updated and improved, and we can place better observational constraints on the mass loss efficiencies.

APPENDIX A: TABLE OF OBSERVED PLANETS

Below we show the planets in each mass bin that we used to form the observed planet points in Figure 9 and Figure 10. Planets marked with a * are transiting planets so their masses are known.

name	M*sin(i) (M_Jup)	a (AU)	e	Age	M*
	0 to <0.3MJ				
GJ 581 c	0.02	0.07	0.16	2.00	0.31
GJ 876 d	0.02	0.02	*0c*	*5.00*	0.32
HD 69830 b	0.03	0.08	0.10	7.00	0.86
GJ 674 b	0.03	0.04	0.20	0.50	0.35
55 Cnc e	0.04	0.04	0.09	7.24	0.91
HD 4308 b	0.05	0.12	0.00	*5.00*	0.90
mu Ara d	0.05	0.09	0.00	3.93	1.15
GJ 581 b	0.05	0.04	0.02	2.00	0.31
HD 190360 c	0.06	0.13	0.01	*5.00*	1.01
HD 219828 b	0.06	0.05	*0c*	*5.00*	1.24
GJ 436 b *	0.07	0.03	0.16	3.00	0.44
HD 49674 b	0.11	0.06	0.09	1.47	1.06
HD 99492 b	0.11	0.12	0.25	3.71	0.86
HD 46375 b	0.23	0.04	0.06	4.96	0.92
HD 76700 b	0.23	0.05	0.10	10.00	1.13
HD 168746 b	0.25	0.07	0.11	9.20	0.93
HD 108147 b	0.26	0.10	0.53	4.40	1.19
HD 109749 b	0.28	0.06	*0c*	*5.00*	1.21
	0.3 to < 0.6 MJ				
HD 88133 b	0.30	0.05	0.13	7.92	1.20
HD 33283 b	0.33	0.15	0.48	*5.00*	1.24
HD 149026 b *	0.36	0.04	*0c*	2.00	1.30
HD 63454 b	0.39	0.04	*0c*	1.00	0.80
HD 212301 b	0.40	0.03	*0c*	*5.00*	1.05
HD 6434 b	0.40	0.14	0.17	7.00	0.79
HD 83443 b	0.40	0.04	0.01	1.79	1.00
BD -10 3166 b	0.46	0.05	0.02	4.18	1.01
HD 75289 b	0.47	0.05	0.03	4.00	1.21
51 Peg b	0.47	0.05	0.01	6.76	1.09
HD 2638 b	0.48	0.04	*0.00*	3.00	0.93
HD 102195 b	0.49	0.05	0.06	2.40	0.93

HD 187123 b	0.53	0.04	0.02	3.80	1.08
OGLE-TR-111b *	0.53	0.05	*0.00*	1.10	0.82
HAT-P-1 b *	0.53	0.06	0.09	3.00	1.16
XO-2b *	0.57	0.04	*0.00*	5.27	0.98
	0.6 to <0.9 MJ				
HAT-P-3 b *	0.60	0.04	*0c*	0.40	0.94
OGLE-TR-10 b *	0.61	0.04	*0.00*	*5.00*	1.10
GJ 876 c	0.62	0.13	0.22	5.00	0.32
HD 27894 b	0.62	0.12	0.05	3.90	0.75
HD 330075 b	0.62	0.04	*0c*	6.20	0.70
HD 209458 b *	0.64	0.05	0.00	4.00	1.10
HAT-P-4b *	0.68	0.04	0.06	4.20	1.26
upsilon And b	0.69	0.06	0.02	3.80	1.32
CoRoT-Exo-4b *	0.73	0.09	0.00	1.00	1.10
55 Cnc b	0.78	0.12	0.02	7.24	0.91
TrES-1 b *	0.80	0.04	*0.00*	2.50	0.89
LUPUS-TR-3b *	0.81	0.05	*0.00*	*5.00*	0.87
TrES-4 *	0.84	0.05	*0.00*	4.70	1.22
HD 38529 b	0.85	0.13	0.25	2.99	1.47
WASP-2 b	0.88	0.03	*0.00*	*5.00*	0.79
WASP-1 b	0.89	0.04	*0.00*	*5.00*	1.15
	0.9 to <1.2 MJ				
XO-1 b *	0.90	0.05	*0.00*	3.60	1.00
HD 179949 b	0.92	0.04	0.02	3.30	1.21
HD 185269 b	0.94	0.08	0.30	4.20	1.28
WASP-7b	0.96	0.06	0.17	*5.00*	1.28
OGLE-TR-182b *	1.01	0.05	*0.00*	*5.00*	1.14
CoRoT-Exo-1b *	1.03	0.03	*0.00*	*5.00*	0.95
OGLE-TR-211b *	1.03	0.05	0.16	*5.00*	1.33
HAT-P-6 b *	1.06	0.05	0.05	2.30	1.29
HAT-P-5b *	1.06	0.04	*0.00*	2.60	1.16
HD 130322 b	1.09	0.09	0.03	1.24	0.89
HD 189733 b	1.13	0.03	0.00	0.60	0.82
OGLE-TR-132b *	1.14	0.03	*0.00*	1.25	1.26
XO-5b *	1.15	0.05	*0.00*	8.50	1.00
	1.2 to <1.5 MJ				
TrES-2 *	1.20	0.04	*0.00*	*5.00*	0.98
WASP-4b *	1.22	0.02	*0.00*	2.00	0.90
OGLE-TR-56 b *	1.29	0.02	*0.00*	0.50	1.17
HD 149143 b	1.30	0.05	*0c*	7.60	1.10

OGLE-TR-113 b *	1.32	0.02	*0.00*	*5.00*	0.78
HD 217107 b	1.41	0.07	0.13	6.50	1.10
	1.5 to <1.8 MJ				
HD 86081 b	1.50	0.03	0.01	*5.00*	1.21
WASP-5b *	1.58	0.03	0.03	3.05	0.99
XO-4b *	1.72	0.06	*0.00*	2.10	1.32
WASP-3 b *	1.76	0.03	0.05	2.10	1.24
HAT-P-7b *	1.78	0.04	*0.00*	2.20	1.47
	1.8 to <2.1 MJ				
HD 68988 b	1.86	0.07	0.12	3.70	1.18
HD 73256 b	1.87	0.04	0.03	0.83	1.05
TrES-3 *	1.92	0.02	*0.00*	*5.00*	0.90
	2.1 to <2.4 MJ				
HD 118203 b	2.14	0.07	0.31	4.60	1.23
	3 to <3.3 MJ				
WASP-10b *	3.06	0.04	0.06	0.80	0.71
	3.3MJ to < 3.6 MJ				
CoRoT-Exo-2b *	3.31	0.03	0.03	*5.00*	0.97
	3.6 to <3.9 MJ				
HD 195019 b	3.69	0.14	0.01	3.90	1.07
HIP 14810 b	3.84	0.07	0.15	*5.00*	0.99
	3.9 to <4.2 MJ				
HD 13445 b	3.91	0.11	0.04	2.94	0.76
tau Boo b	4.13	0.05	0.02	2.40	1.35

The data for these planets are taken from the following references.
(Fuhrmann et al. 1998; Marcy et al. 2000; Brown et al. 2001; McArthur et al. 2004; Pepe et al. 2004; Bonfils et al. 2005; Deming et al. 2005; Fischer et al. 2005; Marcy et al. 2005; Moutou et al. 2005; Rivera et al. 2005; Butler et al. 2006; da Silva et al. 2006; Ge et al. 2006; Gillon et al. 2006; Holman et al. 2006; Johnson et al. 2006a; Johnson et al. 2006b; Lovis et al. 2006; Melo et al. 2006; Bakos et al. 2007a; Bakos et al. 2007b; Bakos et al. 2007c; Bonfils et al. 2007; Burke et al. 2007; Cameron et al. 2007; Fischer et al. 2007; Gillon et al. 2007a; Gillon et al. 2007b; Gillon et al. 2007c; Knutson et al. 2007; Kov·cs et al. 2007; Mandushev et al. 2007; Melo et al. 2007; Minniti et al. 2007; O'Donovan et al. 2007; Pont et al. 2007a; Pont et al. 2007b; Alonso et al. 2008; Anderson et al. 2008; Barge et al. 2008; Burke et al. 2008; Christian et al. 2008; Hellier et al. 2008; Joshi et al. 2008; McCullough et al. 2008; Noyes et al. 2008; Nutzman et al. 2008; P·l et al. 2008; Pollacco et al. 2008)(Rivera et al. 2005; Saffe et al. 2005; Sato et al. 2005; Pont et al. 2007a; Pont et al. 2007b; Takeda et al. 2007; Torres et al. 2007; Udry et al. 2007; Winn et al. 2007a; Winn et al. 2007b; Udalski et al. 2008; Weldrake et al. 2008; Wilson et al. 2008; Winn et al. 2008a; Winn et al. 2008b)

REFERENCES

Alonso, R., M. Auvergne, et al. (2008). "Transiting exoplanets from the CoRoT space mission. II. CoRoT-Exo-2b: a transiting planet around an active G star." Astronomy and Astrophysics **482**: L21-L24.

Anderson, D. R., M. Gillon, et al. (2008). "WASP-5b: a dense, very hot Jupiter transiting a 12th-mag Southern-hemisphere star." Monthly Notices of the Royal Astronomical Society **387**: L4-L7.

Bakos, G., G. Kov·cs, et al. (2007a). "HD 147506b: A Supermassive Planet in an Eccentric Orbit Transiting a Bright Star." Astrophysical Journal **670**: 826-832.

Bakos, G., R. W. Noyes, et al. (2007b). "HAT-P-1b: A Large-Radius, Low-Density Exoplanet Transiting One Member of a Stellar Binary." Astrophysical Journal **656**: 552-559.

Bakos, G., A. Shporer, et al. (2007c). "HAT-P-5b: A Jupiter-like Hot Jupiter Transiting a Bright Star." Astrophysical Journal **671**: L173-L176.

Baraffe, I., F. Selsis, et al. (2004). "The effect of evaporation on the evolution of close-in giant planets." Astronomy & Astrophysics **419**(2): L13-L16.

Barge, P., A. Baglin, et al. (2008). "Transiting exoplanets from the CoRoT space mission. I. CoRoT-Exo-1b: a low-density short-period planet around a G0V star." Astronomy and Astrophysics **482**: L17-L20.

Bell, K. R., P. M. Cassen, et al. (1997). "The Structure and Appearance of Protostellar Accretion Disks: Limits on Disk Flaring." Astrophysical Journal **486**: 372.

Bonfils, X., T. Forveille, et al. (2005). "The HARPS search for southern extra-solar planets." Astronomy & Astrophysics **443**(3): L15-U11.

Bonfils, X., M. Mayor, et al. (2007). "The HARPS search for southern extra-solar planets. X. A m sin i = 11 M_,äï planet around the nearby spotted M dwarf <ASTROBJ>GJ 674</ASTROBJ>." Astronomy and Astrophysics **474**: 293-299.

Brown, T. M., D. Charbonneau, et al. (2001). "Hubble Space Telescope time-series photometry of the transiting planet of HD 209458." Astrophysical Journal **552**(2): 699-709.

Burke, C. J., P. R. McCullough, et al. (2007). "XO-2b: Transiting Hot Jupiter in a Metal-rich Common Proper Motion Binary." Astrophysical Journal **671**: 2115-2128.

Burke, C. J., P. R. McCullough, et al. (2008). XO-5b: A Transiting Jupiter-sized Planet With A Four Day Period.

Burrows, A., I. Hubeny, et al. (2004). "Theoretical radii of transiting giant planets: The case of OGLE-TR-56b." Astrophysical Journal **610**(1): L53-L56.

Butler, R. P., J. T. Wright, et al. (2006). "Catalog of nearby exoplanets." Astrophysical Journal **646**(1): 505-522.

Cameron, A. C., F. Bouchy, et al. (2007). "WASP-1b and WASP-2b: two new transiting exoplanets detected with SuperWASP and SOPHIE." Monthly Notices of the Royal Astronomical Society **375**: 951-957.

Christian, D. J., N. P. Gibson, et al. (2008). WASP-10b: a 3M_J, eccentric transiting gas-giant planet.

da Silva, L., L. Girardi, et al. (2006). "Basic physical parameters of a selected sample of evolved stars." Astronomy and Astrophysics **458**: 609-623.

Del Popolo, A., N. Ercan, et al. (2005). "Orbital migration and the period distribution of exoplanets." Astronomy & Astrophysics **436**(1): 363-372.

Deming, D., S. Seager, et al. (2005). "Infrared radiation from an extrasolar planet." Nature **434**: 740-743.

Fischer, D. A. and J. Valenti (2005). "The Planet-Metallicity Correlation." Astrophysical Journal **622**: 1102-1117.

Fischer, D. A., S. S. Vogt, et al. (2007). "Five Intermediate-Period Planets from the N2K Sample." Astrophysical Journal **669**: 1336-1344.

Fuhrmann, K., M. J. Pfeiffer, et al. (1998). "F- and G-type stars with planetary companions: upsilon Andromedae, rho (1) Cancri, tau Bootis, 16 Cygni and rho Coronae Borealis." Astronomy and Astrophysics **336**: 942-952.

Ge, J., J. van Eyken, et al. (2006). "The First Extrasolar Planet Discovered with a New-Generation High-Throughput Doppler Instrument." Astrophysical Journal **648**: 683-695.

Gillon, M., F. Pont, et al. (2007a). "Detection of transits of the nearby hot Neptune GJ 436 b." Astronomy & Astrophysics **472**(2): L13-L16.

Gillon, M., F. Pont, et al. (2006). "High accuracy transit photometry of the planet OGLE-TR-113b with a new deconvolution-based method." Astronomy and Astrophysics **459**: 249-255.

Gillon, M., F. Pont, et al. (2007b). "The transiting planet OGLE-TR-132b revisited with new spectroscopy and deconvolution photometry[,]." Astronomy and Astrophysics **466**: 743-748.

Gillon, M., A. H. M. J. Triaud, et al. (2007c). Improved parameters for the transiting planet HD 17156b: a high-density giant planet with a very eccentric orbit.

Hellier, C., D. R. Anderson, et al. (2008). WASP-7: The brightest transiting-exoplanet system in the Southern hemisphere.

Holman, M. J., J. N. Winn, et al. (2006). "The Transit Light Curve Project. I. Four Consecutive Transits of the Exoplanet XO-1b." Astrophysical Journal **652**: 1715-1723.

Hubbard, W. B. (1984). Planetary interiors. New York, N.Y., Van Nostrand Reinhold.

Hubbard, W. B., M. F. Hattori, et al. (2007a). "A mass function constraint on extrasolar giant planet evaporation rates." Astrophysical Journal **658**(1): L59-L62.

Hubbard, W. B., M. F. Hattori, et al. (2007b). "Effects of mass loss for highly-irradiated giant planets." Icarus **187**(2): 358-364.

Ida, S. and D. N. C. Lin (2004). "Toward a Deterministic Model of Planetary Formation. I. A Desert in the Mass and Semimajor Axis Distributions of Extrasolar Planets." Astrophysical Journal **604**: 388-413.

Jackson, B., R. Greenberg, et al. (2008a). "Tidal Evolution of Close-in Extrasolar Planets." Astrophysical Journal **678**: 1396-1406.

Jackson, B., R. Greenberg, et al. (2008b). "Tidal Heating of Extrasolar Planets." Astrophysical Journal **681**: 1631-1638.

Johnson, J. A., G. W. Marcy, et al. (2006a). "An Eccentric Hot Jupiter Orbiting the Subgiant HD 185269." Astrophysical Journal **652**: 1724-1728.

Johnson, J. A., G. W. Marcy, et al. (2006b). "The N2K Consortium. VI. Doppler Shifts without Templates and Three New Short-Period Planets." Astrophysical Journal **647**: 600-611.

Joshi, Y. C., D. Pollacco, et al. (2008). WASP-14b: A 7.7 Mjup transiting exoplanet in an eccentric orbit.

Knutson, H. A., D. Charbonneau, et al. (2007). "Using Stellar Limb-Darkening to Refine the Properties of HD 209458b." Astrophysical Journal **655**: 564-575.

Kov·cs, G., G. Bakos, et al. (2007). "HAT-P-4b: A Metal-rich Low-Density Transiting Hot Jupiter." Astrophysical Journal **670**: L41-L44.

Lammer, H., F. Selsis, et al. (2003). "Atmospheric loss of exoplanets resulting from stellar X-ray and extreme-ultraviolet heating." Astrophysical Journal **598**(2): L121-L124.

Lin, D. N. C., P. Bodenheimer, et al. (1996). "Orbital migration of the planetary companion of 51 Pegasi to its present location." Nature **380**: 606-607.

Liu, X., A. Burrows, et al. (2008). Theoretical Radii of Extrasolar Giant Planets: the Cases of TrES-4, XO-3b, and HAT-P-1b.

Lovis, C., M. Mayor, et al. (2006). "An extrasolar planetary system with three Neptune-mass planets." Nature **441**(7091): 305-309.

Mandushev, G., F. T. O'Donovan, et al. (2007). "TrES-4: A Transiting Hot Jupiter of Very Low Density." Astrophysical Journal **667**: L195-L198.

Marcy, G., R. P. Butler, et al. (2005). "Observed properties of exoplanets: Masses, orbits, and metallicities." Progress of Theoretical Physics Supplement(158): 24-42.

Marcy, G. W., R. P. Butler, et al. (2000). "Sub-saturn planetary candidates of HD 16141 and HD 46375." Astrophysical Journal **536**(1): L43-L46.

McArthur, B. E., M. Endl, et al. (2004). "Detection of a Neptune-mass planet in the rho(1) Cancri system using the Hobby-Eberly telescope." Astrophysical Journal **614**(1): L81-L84.

McCullough, P. R., C. J. Burke, et al. (2008). XO-4b: An Extrasolar Planet Transiting an F5V Star.

Melo, C., N. C. Santos, et al. (2007). "A new Neptune-mass planet orbiting HD 219828." Astronomy and Astrophysics **467**: 721-727.

Melo, C., N. C. Santos, et al. (2006). "On the age of stars harboring transiting planets." Astronomy and Astrophysics **460**: 251-256.

Minniti, D., J. M. Fern·ndez, et al. (2007). "Millimagnitude Photometry for Transiting Extrasolar Planetary Candidates. III. Accurate Radius and Period for OGLE-TR-111-b." Astrophysical Journal **660**: 858-862.

Moutou, C., M. Mayor, et al. (2005). "The HARPS search for southern extra-solar planets. IV. Three close-in planets around HD 2638, HD 27894 and HD 63454." Astronomy and Astrophysics **439**: 367-373.

Noyes, R. W., G. Bakos, et al. (2008). "HAT-P-6b: A Hot Jupiter Transiting a Bright F Star." Astrophysical Journal **673**: L79-L82.

Nutzman, P., D. Charbonneau, et al. (2008). A Precise Estimate of the Radius of the Exoplanet HD 149026b from Spitzer Photometry.

O'Donovan, F. T., D. Charbonneau, et al. (2007). "TrES-3: A Nearby, Massive, Transiting Hot Jupiter in a 31 Hour Orbit." Astrophysical Journal **663**: L37-L40.

P·l, A., G. Bakos, et al. (2008). "HAT-P-7b: An Extremely Hot Massive Planet Transiting a Bright Star in the Kepler Field." Astrophysical Journal **680**: 1450-1456.

Pepe, F., M. Mayor, et al. (2004). "The HARPS search for southern extra-solar planets. I. HD 330075 b: A new ``hot Jupiter"." Astronomy and Astrophysics **423**: 385-389.

Pollacco, D., I. Skillen, et al. (2008). "WASP-3b: a strongly irradiated transiting gas-giant planet." Monthly Notices of the Royal Astronomical Society **385**: 1576-1584.

Pont, F., C. Moutou, et al. (2007a). "The "666" collaboration on OGLE transits. I. Accurate radius of the planets OGLE-TR-10b and OGLE-TR-56b with VLT deconvolution photometry." Astronomy and Astrophysics **465**: 1069-1074.

Pont, F., O. Tamuz, et al. (2007b). A transiting planet among 23 new near-threshold candidates from the OGLE survey - OGLE-TR-182.

Raymond, S. N., R. Barnes, et al. (2008). "Observable consequences of planet formation models in systems with close-in terrestrial planets." Monthly Notices of the Royal Astronomical Society **384**: 663-674.

Ribas, I., E. F. Guinan, et al. (2005). "Evolution of the solar activity over time and effects on planetary atmospheres. I. High-energy irradiances (1-1700 angstrom)." Astrophysical Journal **622**(1): 680-694.

Rivera, E. J., J. J. Lissauer, et al. (2005). "A similar to 7.5 M-circle plus planet orbiting the nearby star, GJ 876." Astrophysical Journal **634**(1): 625-640.

Saffe, C., M. GÛmez, et al. (2005). "On the ages of exoplanet host stars." Astronomy and Astrophysics **443**: 609-626.

Sato, B., D. A. Fischer, et al. (2005). "The N2K consortium. II. A transiting hot Saturn around HD 149026 with a large dense core." Astrophysical Journal **633**(1): 465-473.

Saumon, D., G. Chabrier, et al. (1995). "AN EQUATION OF STATE FOR LOW-MASS STARS AND GIANT PLANETS." Astrophysical Journal Supplement Series **99**(2): 713-741.

Takeda, G., E. B. Ford, et al. (2007). "Structure and evolution of nearby stars with planets. II. Physical properties of similar to 1000 cool stars from the SPOCS Catalog." Astrophysical Journal Supplement Series **168**(2): 297-318.

Torres, G., G. Bakos, et al. (2007). "HAT-P-3b: A Heavy-Element-rich Planet Transiting a K Dwarf Star." Astrophysical Journal **666**: L121-L124.

Trilling, D. E., W. Benz, et al. (1998). "Orbital evolution and migration of giant planets: Modeling extrasolar planets." Astrophysical Journal **500**(1): 428-439.

Udalski, A., F. Pont, et al. (2008). "OGLE-TR-211 - a new transiting inflated hot Jupiter from the OGLE survey and ESO LP666 spectroscopic follow-up program." Astronomy and Astrophysics **482**: 299-304.

Udry, S., X. Bonfils, et al. (2007). "The HARPS search for southern extra-solar planets. XI. Super-Earths (5 and 8 M{,äï}) in a 3-planet system." Astronomy and Astrophysics **469**: L43-L47.

Vidal-Madjar, A., A. Lecavelier des Etangs, et al. (2003). "An extended upper atmosphere around the extrasolar planet HD209458b." Nature **422**: 143-146.

Watson, A. J., T. M. Donahue, et al. (1981). "THE DYNAMICS OF A RAPIDLY ESCAPING ATMOSPHERE - APPLICATIONS TO THE EVOLUTION OF EARTH AND VENUS." Icarus **48**(2): 150-166.

Weldrake, D. T. F., D. D. R. Bayliss, et al. (2008). "Lupus-TR-3b: A Low-Mass Transiting Hot Jupiter in the Galactic Plane?" Astrophysical Journal **675**: L37-L40.

Wilson, D. M., M. Gillon, et al. (2008). "WASP-4b: A 12th Magnitude Transiting Hot Jupiter in the Southern Hemisphere." Astrophysical Journal **675**: L113-L116.

Winn, J. N., J. Asher Johnson, et al. (2008a). The Prograde Orbit of Exoplanet TrES-2b.

Winn, J. N., M. J. Holman, et al. (2007a). "The Transit Light Curve Project. V. System Parameters and Stellar Rotation Period of HD 189733." Astronomical Journal **133**: 1828-1835.

Winn, J. N., M. J. Holman, et al. (2007b). "The Transit Light Curve Project. III. Tres Transits of TrES-1." Astrophysical Journal **657**: 1098-1106.

Winn, J. N., M. J. Holman, et al. (2008b). The Transit Light Curve Project. IX. Evidence for a Smaller Radius of the Exoplanet XO-3b.

Wittenmyer, R. A., M. Endl, et al. (2006). "Detection Limits from the McDonald Observatory Planet Search Program." Astronomical Journal **132**: 177-188.

Yelle, R. V. (2004). "Aeronomy of extra-solar giant planets at small orbital distances." Icarus **170**(1): 167-179.

Yelle, R. V. (2006). "Aeronomy of extra-solar giant planets at small orbital distances (vol 170, pg 167, 2004)." Icarus **183**(2): 508-508.